Evaluation of subleading β decay matrix elements in light nuclei

Author: Manuel Carrera Moreno
Facultat de Física, Universitat de Barcelona, Diagonal 645, 08028 Barcelona, Spain.

Advisor: Javier Menéndez

Abstract: β decay is the process most nuclei go through in order to become more stable. The goal of this work is to obtain a more precise theoretical prediction of the half live of the ^{23}Ne to ^{23}Na β decay. After calculating the wavefunctions corresponding to ^{23}Ne and ^{23}Na using the shell model code *Nathan*, I evaluate the nuclear matrix element of a subleading β decay operator for the first time. This correction reduces the half lives of the decay branches studied up to 3%.

I. INTRODUCTION

A. Motivations

When some process is described theoretically, initially it is done in a simple way in order to understand its main features. In a second step, the goal is to improve the model in order to gain precision and reproduce better the experimental results. The Standard Model is one of the widest theories that mankind has ever created. To test if its predictions agree with experiments, one thing that one can do is to make high precision experiments and compare them to the theoretical results, which have to be also precise. This is doable in the case of the β decay [1], a process that occurs in nearly all the nuclei [2] (except the heavier ones). This work calculates more precisely the half live and the decay probability of some possible decays between ^{23}Ne and ^{23}Na, transitions which are expected to be measured with high precision in the near future.

B. Beta Decay

β decay are not one but several possible processes: β^-, β^+ and electron capture (EC):

$$\beta^- : n \longrightarrow p + e^- + \bar{\nu}_e, \tag{1}$$

$$\beta^+ : p \longrightarrow n + e^+ + \nu_e, \tag{2}$$

$$EC : p + e^- \longrightarrow n + \nu_e. \tag{3}$$

Since the neutron n is slightly more massive than the proton p, (1) can happen in the vacuum for a free neutron, but (2) cannot. Here e^- and ν_e are the electron and the electronic neutrino, while e^+ and $\bar{\nu_e}$ are their respective antiparticles.

There are two leading types of β decays: if the projection of the spin of the nucleon involved remains the same, then it is a Fermi β decay; if there is a shift, then it is a Gamow-Teller β decay. Since both are available decay channels, the β decay half live of a nucleus involves both processes:

$$t_{1/2} = \frac{\kappa}{f_0(B_F + B_{GT})}, \tag{4}$$

Where $\kappa = 6147s$, f_0 is a phase integral involving the lepton kinematics and B_F and B_{GT} are the reduced transition probabilities of the Fermi and the Gamow-Teller β decay, respectively. Those reduced transition probabilities depend directly on the reduced matrix elements of the Fermi and Gamow-Teller transition operators:

$$B_F = \frac{g_V^2}{2J_i + 1}|M_F|^2, \tag{5}$$

$$B_{GT} = \frac{g_A^2}{2J_i + 1}|M_{GT}|^2. \tag{6}$$

Where $g_V = 1.0$ is the vector coupling constant and $g_A = 1.27$ is the axial-vector coupling constant. J_i is the initial angular momentum. In turn, the reduced matrix elements depend on the reduced single-particle matrix elements (evaluated between single-particle states) $M_F(ab)$ and $M_{GT}(ab)$:

$$\begin{aligned} M_F =& (J_f, T_f \parallel \sum_j \mathbb{I}_j \tau_j^{\pm} \parallel J_i, T_i) \\ =& \delta_{J_i, J_f} \sum_{ab} M_F(ab) \cdot (J_f, T_f \parallel [c_a^\dagger c_b]_0 \parallel J_i, T_i), \end{aligned} \tag{7}$$

$$\begin{aligned} M_{GT} =& (J_f, T_f \parallel \sum_j \sigma_{\mathbf{j}} \tau_{\mathbf{j}}^{\pm} \parallel J_i, T_i) \\ =& \sum_{ab} M_{GT}(ab) \cdot (J_f, T_f \parallel [c_a^\dagger c_b]_1 \parallel J_i, T_i). \end{aligned} \tag{8}$$

Here, $c_a^\dagger$ is called a creation operator, since it creates a particle in the state a, and c_b is a annihilation operator, since it destroys a particle in the state b. They define the one-body transition density. σ represents the spin and $\tau^\pm$ are the isospin operators that transform a neutron into a proton (-) or viceversa (+). Also, T_i and T_f are the initial and final isospin and J_f is the final total angular momentum. In this work I will evaluate reduced single-particle matrix elements for operators beyond the Fermi and Gamow-Teller ones.

C. Shell Model

A nucleus is a system of Z protons and N neutrons that interact with each other mainly via the strong in-

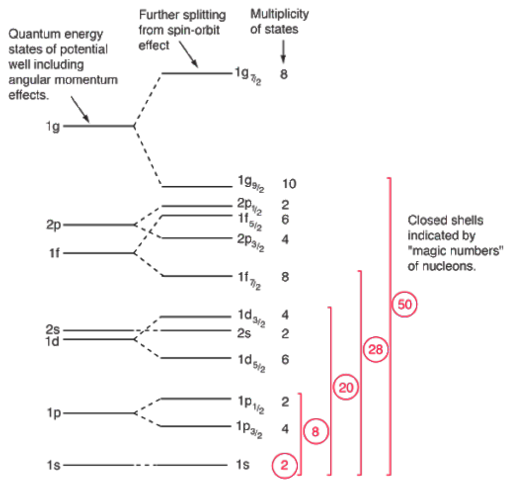

FIG. 1: Harmonic oscillator single-particle levels. Initially the energy levels depend exclusively on n and l, and when the spin-orbit coupling is applied, those levels split in two. Large energy gaps divide the spectrum in shells. From [3].

teraction. In other words it is a system of $A = N + Z$ fermions that strongly interact with each other. Restricting to two-body interactions, the Schrödinger equation to solve reads

$$\Big[\sum_i \frac{-\hbar^2\nabla_i^2}{2m_i} + \sum_{i<j} V(\vec{r_i},\vec{r_j})\Big]\Psi(\vec{r_1},...,\vec{r_A}) = E\Psi(\vec{r_1},...,\vec{r_A}). \tag{9}$$

The first term is the kinetic energy, the second one is the interaction between nucleons, E is the total energy of the system and Ψ is the wavefunction. The system can be approached defining a mean field as

$$H = T + \sum_i v(\vec{r_i}) + V - \sum_i v(\vec{r_i}) = T + \sum_i v(\vec{r_i}) + V_{RES} \tag{10}$$

In this case, the first two terms of the hamiltonian define a mean field that can be described with one-body potentials, such as the harmonic oscillator. Its eigenvalues are called the single-particle energies of orbitals. Adding a spin-orbit coupling term, the magic numbers, numbers of protons and/or neutrons at which nuclei become very stable (corresponding to large energy gaps in the shell model) are well reproduced.

On the other hand, V_{RES} contains all the interaction between nucleons. I will obtain the wavefunctions of ^{23}Ne and ^{23}Na within the shell model. In particular, I will use the code *Nathan* [4] and the interactions USD and USDB [5]. What one can see from experiments is that a closed shell has a total angular momentum J=0. This makes things easier, because if a nucleus has a closed shell, its contribution to the total angular momentum will be none, and in addition, its nucleons would not likely occupy more energetic levels because their configuration is very stable. In fact, in the shell model the low energy nucleons are approximated to form a core, which is represented by a single Slater determinant. The rest of the nucleons are approximated to be in the valence space, the next shell over the core, represented by a linear combination of Slater determinants. Higher shells are neglected. This does not mean that the core must be neglected, since its interaction with the valence space leads to an effective hamiltonian, so that the equation to solve is [6]

$$H_{eff} \mid J,T\rangle = E \mid J,T\rangle, \tag{11}$$

with H_{eff} being the version of H that operates in the valence space considered. In this work, the core will be a ^{16}O nucleus (8 protons and 8 neutrons) and the *valence space* will be the *sd* shell (i.e. the orbitals with n=0 and l=2 and the orbital with n=1 and l=0, being n the principal quantum number and l the orbital angular momentum quantum number. Therefore, the valence space used in this work lies between the magic numbers $N = Z = 8$ and $N = Z = 20$, as shown in Fig. 1.

D. Angular momenta and spherical tensors

The spin and the relative motion between nucleons are angular momenta, and the angular momentum of a system is the result of coupling all the angular momenta of the components of the system [2]. Starting with a system of two well-defined angular momenta $|j_1, m_1\rangle$ and $|j_2, m_2\rangle$,

$$\begin{aligned}|j_1, j_2; j, m\rangle &= \sum_{m_1,m_2} (j_1, m_1, j_2, m_2|j, m)|j_1, m_1, j_2, m_2\rangle \\ &= \sum_{m_1,m_2} (-1)^{j_1-j_2+m}\hat{j}\begin{pmatrix} j_1 & j_2 & j \\ m_1 & m_2 & -m\end{pmatrix}|j_1, m_1, j_2, m_2\rangle\end{aligned} \tag{12}$$

where $|j_1 - j_2| < j < j_1 + j_2$ is the coupled angular momentum, $m = m_1 + m_2$ its projection and $\hat{j} = \sqrt{2j+1}$ with Clebsch-Gordan coefficients $(j_1, m_1, j_2, m_2|j, m)$, and their alternative definition, the *3j-symbols* which is the object in parenthesis in (12). In the case of coupling 3 angular momenta the total angular momenta does not depend on the coupling order but so do the states [2]. The change from the basis generated in one order to another can be done by using the *6j-symbols*:

$$\begin{aligned}&|j_2, j_3(j_{23}), j_1; j, m\rangle = \\ &\sum_{j_{12}} (-1)^{j_1+j_2+j_3+j}\hat{j_{12}}\hat{j_{23}}\begin{Bmatrix} j_1 & j_2 & j_{12} \\ j_3 & j & j_{23}\end{Bmatrix}|j_1, j_2(j_{12}), j_3; j, m\rangle\end{aligned} \tag{13}$$

Similarly, but with the coupling of 4 angular momenta, there are the *9j-symbols* that appear in (18).

Spherical tensor operators $\mathbf{T}_L$ are a special type of operators which have components (like vectors) that are operators themselves. Specifically, a spherical tensor has

$2L+1$ components: T_{LM}. L is the angular momentum (also named *rank*) of the spherical tensor and M is its $\hat{z}$ axis projection. In fact, $\vec{J}$ is a spherical tensor itself of angular momentum 1 (its components are J_{+1}, J_0, J_{-1}), such as the position $\vec{r}$. The isospin $\vec{\tau}$ is also a spherical tensor with components $\tau_{+1}, \tau_0, \tau_{-1}$. Likewise angular momenta, spherical tensors can also be coupled to a certain total momentum:

$$[\mathbf{T}_{L_1}, \mathbf{S}_{L_2}]_{LM} = T_{LM} = \sum_{M_1,M_2} (L_1, M_1, L_2, M_2|L, M) T_{L_1,M_1} S_{L_2,M_2}. \tag{14}$$

The reduced matrix element of a tensor operator is defined via the Wigner-Eckart theorem:

$$\langle \xi' j' m' | T_{LM} | \xi j m \rangle = \hat{j'}^{-1} (jmLM|j'm')(\xi' j \parallel \mathbf{T}_L \parallel \xi j), \tag{15}$$

where ξ represents the additional quantum numbers. Note that reduced matrix elements do not depend on the projection. Here are two of them that will be enough for our calculations:

$$(j' \parallel \mathbb{I} \parallel j) = \delta_{j,j'} \hat{j}, \tag{16}$$

$$(j' \parallel \mathbf{J} \parallel j) = \delta_{j,j'} \hbar \sqrt{j(j+1)(2j+1)}, \tag{17}$$

In fact, the identity is a spherical tensor of rank 0. Another expression I use is the following

$$(j_1 j_2 j \parallel \mathbf{T}_L \parallel j_1' j_2' j') = \tag{18}$$
$$\hat{j}\hat{j'}\hat{L} \begin{Bmatrix} j_1 & j_2 & j \\ j_1' & j_2' & j' \\ L_1 & L_2 & L \end{Bmatrix} \cdot (j_1 \parallel \mathbf{T}_{L_1} \parallel j_1')(j_2 \parallel \mathbf{S}_{L_2} \parallel j_2'),$$

where $T_{LM} = [\mathbf{T}_{L_1}, \mathbf{S}_{L_2}]_{LM}$. Here, $\mathbf{T}_{L_1}$ operates in the $|j_1, m_1\rangle$ space and $\mathbf{S}_{L_2}$ operates in the $|j_2, m_2\rangle$ space.

II. DEVELOPING SECTIONS

This work has two main contributions: one analytical and another numerical. In particular, I have obtained new results for the single-particle matrix elements, and implemented a new subroutine for the most relevant β decay correction into the shell model code *Nathan*.

In this work I focus on the β decay

$$^{23}_{10}\mathrm{Ne} \longrightarrow {}^{23}_{11}\mathrm{Na} + e^- + \bar{\nu}_e, \tag{19}$$

which begins in the ground state of ^{23}Ne, with total angular momentum J=5/2 and a positive parity. It ends in four possible states of the ^{23}Na: its ground state, with J=3/2 and 3 excited states, with J= 3/2, 5/2 and 7/2. All states have positive parity. The experimental energy for all those states is very well determined [7], but I will also calculate them numerically to test the quality of my calculations.

For these transitions $M_F = 0$, because the lowest lying state of the ^{23}Ne has an isospin T=3/2, while for the low energy states of ^{23}Na T=1/2, and $\sum_j \tau_j^-$ does not connect states with different isospin. Therefore $\sum_j \tau_j^-$ only connects with the T=3/2, T_z=1/2 and $J^P = \frac{5}{2}^+$, which is at higher energy than the ^{23}Ne ground state as shown in Fig. 2. That implies that $B_F = 0$ in (4).

Recently, [7] has introduced an improved expression for the β decay of ^{23}Ne:

$$t_{1/2}^{-1} = \frac{f_0}{\kappa} B_{GT} (1 + \delta_{shape}). \tag{20}$$

This equation takes into account the nuclear shape and helps me to be more precise in the calculations of the transition probabilities. The shape correction is [7]

$$\delta_{shape} \approx \frac{2}{3} Q_\beta \Big[\sqrt{2} \frac{(f \parallel \hat{M}_1^V/q \parallel i)}{(f \parallel \hat{L}_1^A \parallel i)} - \frac{(f \parallel \hat{C}_1^A/q \parallel i)}{(f \parallel \hat{L}_1^A \parallel i)} \Big], \tag{21}$$

with β decay operators [7]

$$\hat{L}_1^A(q) = \frac{i g_A}{2\sqrt{3\pi}} \sum_j \vec{\sigma_j} \tau_j^\pm, \tag{22}$$

$$\hat{C}_0^V(q) = \frac{g_V}{2\sqrt{\pi}} \sum_j \tau_j^\pm, \tag{23}$$

$$\hat{M}_1^V(q) = \frac{i}{2\sqrt{6\pi}} \frac{q}{m_N} \sum_j [g_V \vec{L_j} + \mu \vec{\sigma_j}] \tau_j^\pm, \tag{24}$$

$$\hat{C}_1^A(q) = -\frac{i g_A}{2\sqrt{3\pi}} \frac{q}{m_N} \sum_j [\vec{r_j}(\vec{\sigma_j} \cdot \vec{\nabla}_j) + \frac{1}{2}\vec{\sigma_j}] \tau^\pm, \tag{25}$$

$$\hat{L}_0^V(q) = -\frac{g_V}{12\sqrt{\pi}} \frac{q}{m_N} \sum_j [3 + 2\vec{r_j} \cdot \vec{\nabla}_j] \tau_j^\pm. \tag{26}$$

Here $Q_\beta = m(^{23}\mathrm{Ne}) - m(^{23}\mathrm{Na}) - m_e$ is the energy released in the β decay, where m denotes the mass. $\mu \simeq 4.706$ is the isovector magnetic moment and q is the transferred linear momentum. The first two operators (Gamow-Teller and Fermi) appear at leading order, while the other three are smaller since they are inversely proportional to the nucleon mass: $\frac{q}{m_N} \approx \frac{Q_\beta}{m_N}$. I have identified $q \approx Q_\beta$ since in the two extreme scenarios (the electron or the antineutrino keeping all the kinetic energy) and in the symmetric one the approximation is better than 30%.

In order to evaluate these operators I will need to calculate first the initial and final states, which I obtain using the shell model code *Nathan*. Fig. 2 shows the results in comparison to experiment. The two calculations correspond to two different H_{eff}: USD and USDB [5]. USD is a little bit more accurate than USDB. In any case, the difference between the calculations and the experiment do not exceed 0.2 MeV, so that the calculated excited energies are very accurate for the three lower excited states.

Once I have the initial and final states, I need to evaluate the reduced single-particle matrix elements as shown in (7) and (8). The Fermi and Gamow-Teller ones are

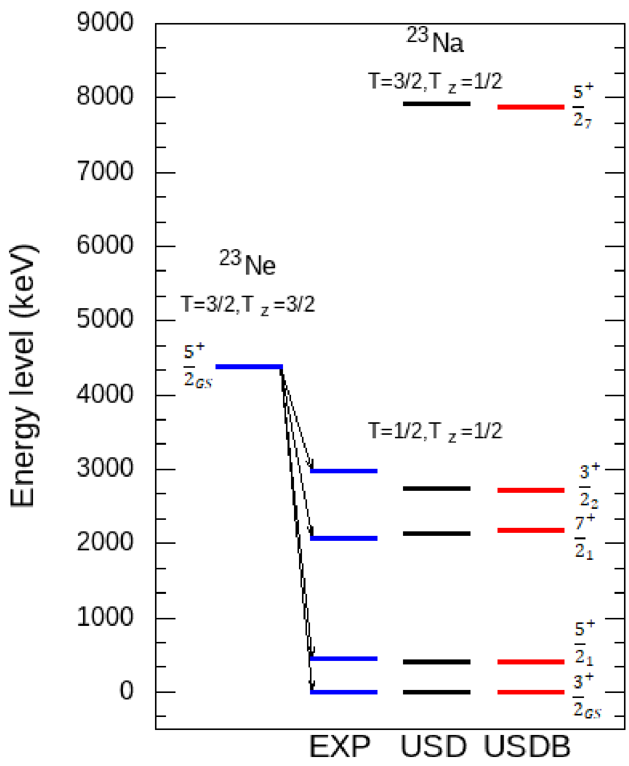

FIG. 2: Shell model spectrum calculations and experimental result for the ground state and four excited states of ^{23}Na. The left line represents the initial ^{23}Ne state, placed at the Q_β value of the transition. The ^{23}Na states are placed relatively to it, with the ground state at the origin.

well known:

$$(n_f, l_f, \frac{1}{2}, j_f \parallel \mathbb{I} \parallel n_i, l_i, \frac{1}{2}, j_i) = \delta_{n_i,n_f}\delta_{l_i,l_f}\delta j_i, j_f \hat{j}_i \quad (27)$$

$$(n_f, l_f, \frac{1}{2}, j_f \parallel \sigma \parallel n_i, l_i, \frac{1}{2}, j_i) = \quad (28)$$
$$\sqrt{6}\delta_{n_i,n_f}\delta_{l_i,l_f}\hat{j}_i\hat{j}_f(-1)^{l_f+j_f+\frac{3}{2}} \begin{Bmatrix} \frac{1}{2} & \frac{1}{2} & 1 \\ j_i & j_f & l_f \end{Bmatrix}.$$

In addition, in (24)-(26) there are new operators. First of all, there is the $\mathbf{L}$ operator. It does not affect the radial part and describes how the angular momentum of the nucleon involved in the decay affects the transition probability. Using (18), I obtain:

$$(n_f, l_f, \frac{1}{2}, j_f \|\mathbf{L}\| n_i, l_i, \frac{1}{2}, j_i) = \delta_{n_i,n_f}\delta_{l_i,l_f} \times \quad (29)$$
$$\hat{j}_i\hat{j}_f\hbar\sqrt{l_f(l_f+1)(2l_f+1)}(-1)^{3/2+l_f+j_i} \begin{Bmatrix} l_f & l_i & 1 \\ j_i & j_f & \frac{1}{2} \end{Bmatrix},$$

On the other hand, the last two operators $\mathbf{r}\cdot\nabla$ and $\mathbf{r}(\sigma\cdot\nabla)$ operate on the radial part. These two operators are related to the recoil that the nucleus suffers due to momentum conservation. With the help of [8] and using (14), I have found the reduced single-particle matrix elements:

	$(f\|\|\vec{\sigma}\,\tau^-\|\|i)$	$(f\|\|\vec{L}\,\tau^-\|\|i)$
$(\frac{5}{2})^+_{GS} \to (\frac{3}{2})^+_{GS}$	0,30 (2)	2,52 (2)
$(\frac{5}{2})^+_{GS} \to (\frac{3}{2})^{+*}_2$	0,213 (3)	0,057 (7)
$(\frac{5}{2})^+_{GS} \to (\frac{5}{2})^+_1$	0,32 (3)	1,96 (3)
$(\frac{5}{2})^+_{GS} \to (\frac{7}{2})^+_1$	0,085 (6)	1,14 (2)
	$(f\|\|\hat{L}^A_1\|\|i)$	$(f\|\|\hat{M}^V_1\|\|i)$
$(\frac{5}{2})^+_{GS} \to (\frac{3}{2})^+_{GS}$	0,063 (5)	0,00213 (6)
$(\frac{5}{2})^+_{GS} \to (\frac{3}{2})^{+*}_2$	0,04537 (7)	0,000186 (1)
$(\frac{5}{2})^+_{GS} \to (\frac{5}{2})^+_1$	0,066 (5)	0,00167 (8)
$(\frac{5}{2})^+_{GS} \to (\frac{7}{2})^+_1$	0,018 (2)	0,000435 (3)

TABLE I: Value of the reduced matrix elements for the main operators in the ^{23}Ne to ^{23}Na β decay.

$$(n_f, l_f, \frac{1}{2}, j_f \|\mathbf{r}\cdot\nabla\| n_i, l_i, \frac{1}{2}, j_i) = \quad (30)$$
$$-\sqrt{3}\hat{j}_i \langle n_f, l_f, j_f | r\frac{d}{dr} | n_i, l_i, j_i \rangle,$$

$$(n_f, l_f, \frac{1}{2}, j_f \|\mathbf{r}\cdot(\sigma\cdot\nabla)\| n_i, l_i, \frac{1}{2}, j_i) = \quad (31)$$
$$-\sqrt{3}(-1)^{l_i+1}\cdot\hat{j}_i\hat{j}_f \frac{1+(-1)^{l_f-l_i}}{2} \begin{pmatrix} j_i & j_f & 1 \\ \frac{1}{2} & -\frac{1}{2} & 0 \end{pmatrix}$$
$$\times\Big[\delta_{j_i,l_i+\frac{1}{2}}\cdot l_i\cdot\delta_{n_i,n_f} + \delta_{j_i,l_i-\frac{1}{2}}\cdot(l_i+1)\delta_{n_i,n_f}$$
$$-(\delta_{j_i,l_i+\frac{1}{2}} - \delta_{j_i,l_i-\frac{1}{2}})\langle n_f, l_f, j_f | r\frac{d}{dr} | n_i, l_i, j_i \rangle\Big].$$

Both elements depend on the radial operator $r\frac{d}{dr}$. Assuming the radial harmonic oscillator single particle stats, then (30) and (31) become:

$$(n_f, l_f, \frac{1}{2}, j_f \|\mathbf{r}\cdot\nabla\| n_i, l_i, \frac{1}{2}, j_i) = \quad (32)$$
$$-\sqrt{3}\hat{j}_i\cdot\Big[l_i\langle n_f, l_f \mid n_i, l_i\rangle - \sqrt{n_i^2 - n_i}\langle n_f, l_f \mid n_i - 2, l_i + 2\rangle$$
$$+\sqrt{(n_i+l_i+3/2)\cdot(n_i+l_i+5/2)}\langle n_f, l_f \mid n_i, l_i+2\rangle\Big],$$
$$(n_f, l_f, \frac{1}{2}, j_f \|\mathbf{r}\cdot(\sigma\cdot\nabla)\| n_i, l_i, \frac{1}{2}, j_i) = \quad (33)$$
$$-\sqrt{3}(-1)^{l_i+1}\cdot\hat{j}_i\hat{j}_f \frac{1+(-1)^{l_f-l_i}}{2} \begin{pmatrix} j_i & j_f & 1 \\ \frac{1}{2} & -\frac{1}{2} & 0 \end{pmatrix}$$
$$\times\Big[(2l_i+1)\delta_{j_i,l_i-\frac{1}{2}}\langle n_f, l_f \mid n_i, l_i\rangle - (\delta_{j_i,l_i+\frac{1}{2}} - \delta_{j_i,l_i-\frac{1}{2}})$$
$$\cdot(\sqrt{(n_i+l_i+3/2)\cdot(n_i+l_i+5/2)}\langle n_f, l_f \mid n_i, l_i+2\rangle$$
$$-\sqrt{n_i^2 - n_i}\langle n_f, l_f \mid n_i - 2, l_i + 2\rangle)\Big].$$

Finally, the reduced matrix elements are given by a combination of single-particle matrix elements and the

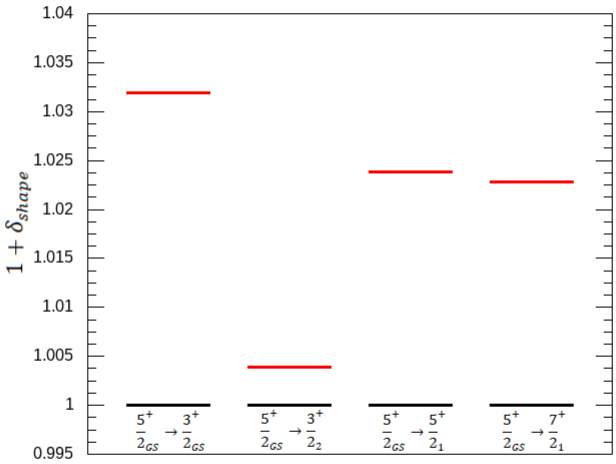

FIG. 3: Normalized reduced transition probability with (red) and without the shape correction (black).

one-body transition density:

$$(J_f, T_f \parallel \sum_j \mathbf{T}_{\lambda j}\tau_j^{\pm} \parallel J_i, T_i) = \qquad (34)$$
$$\hat{\lambda}^{-1}\sum_{ab}(a \parallel \mathbf{T}_\lambda \parallel b)\cdot(J_f, T_f \parallel [c_a^\dagger c_b]_1 \parallel J_i, T_i).$$

In addition to the matrix elements reduced in the angular momentum space, the isospin can be treated also as a t=1/2 angular momentum, with projections t_z=-1/2 for the proton and t_z=1/2 for the neutron. In β^- decay we are "changing" a neutron for a proton, so we need to operate with the -1 projection of the isospin operator: $\langle \frac{1}{2}, -\frac{1}{2} \mid \tau^- \mid \frac{1}{2}, \frac{1}{2}\rangle = \frac{1}{\sqrt{2}}\langle \frac{1}{2}, -\frac{1}{2} \mid \tau_{-1} \mid \frac{1}{2}, \frac{1}{2}\rangle = 1$. This change of a neutron into a proton is represented by the one-body transition density operator in (7), (8) and (34).

Using the Gamow-Teller matrix element already implemented in *Nathan* and my implementation of the **L** matrix element, I evaluate (22) and (24). Table I shows the results. I have checked the numerical results for (24) comparing them to electromagnetic transitions [9] using the Wigner-Eckart theorem (in a electromagnetic transition the isospin does not change, so that the isospin operator is τ^0 instead of τ^-)

$$\langle T_f = \frac{1}{2}, T_{z_f} = \frac{1}{2} \mid \sum_j \mathbf{L}_j \tau_j^- \mid T_i = \frac{3}{2}, T_{z_i} = \frac{3}{2}\rangle = \qquad (35)$$
$$\frac{1}{\sqrt{2}}\frac{(\frac{3}{2},\frac{3}{2},1,-1 \mid \frac{1}{2},\frac{1}{2})}{(\frac{1}{2},\frac{1}{2},1,0 \mid \frac{3}{2},\frac{1}{2})}\langle \frac{3}{2}, \frac{1}{2} \mid \sum_j \mathbf{L}_j \tau_j^0 \mid \frac{1}{2}, \frac{1}{2}\rangle =$$
$$\frac{1}{\sqrt{6}}\langle T_f = \frac{3}{2}, T_{z_f} = \frac{1}{2} \mid \sum_j \mathbf{L}_j \tau_j^0 \mid T_i = \frac{1}{2}, T_{z_i} = \frac{1}{2}\rangle,$$

where the initial state in the electromagnetic transitions is the T=3/2, T_z=1/2 and J=5/2 state in ^{23}Na shown in Fig. 2 as the highest excited state.

Fig. 3 summarizes the correction to the half live of the subleading term in the transitions studied in ^{23}Ne. The δ_{shape} correction is in every case of the order of 1%. It is specially small in the case of the $\frac{5}{2}^+_{GS} \longrightarrow \frac{3}{2}^+_2$ transition where it amounts to $\approx 0.5\%$, while in the other cases it is $\approx 3\%$.

III. CONCLUSIONS

USD and USDB interactions are pretty accurate in reproducing experimental spectra. I have calculated a correction on the half live of the ^{23}Ne to ^{23}Na β decay. This correction is about 3%, so it should be taken into account when comparing to high precision experiments such as [1]. In this work, the second term in (21) has not been treated due to lack of time. Nevertheless, it could be very interesting to calculate this additional correction in future work.

Acknowledgments

Thanks to Javier Menéndez, the advisor of this work, for how much he has helped me in all this path. Thank you to my family for letting me arrive to this moment and to my friends for distracting me when I was blocked and make me forget all my problems.

[1] H. Rahangdale H. et al., (2018). *Branching ratio measurement in ^{23}Ne Beta decay* HNPS Advances in Nuclear Physics, Vol.26, 31-36
[2] J. Suhonen, (2007). *From Nucleons to Nucleus.* Springer, Jyväskylä, Findland.
[3] *hyperphysics.phy-astr.gsu.edu/hbase/Nuclear/shell.html. Hyperphysics.*
[4] E. Caurier et al., (2005). *The shell model as a unified view of nuclear structure.* Reviews of Modern Physics, Vol. 77, 427-445
[5] W. A. Richter, S. Mkhize & B. A. Brown, (2008). *sd-shell observables for the USDA and USDB Hamiltonians,* Physical Review, Vol. 78, 064302.
[6] A. Poves & F. Nowacki, (2001). *An Advanced Course in Modern Nuclear Physics.* Springer-Verlag. 70-86.
[7] D. Gazit & A. Glick-Magid, (2020). *Beta Decay of Ne-23.* Private communication.
[8] T. W. Donnelly & W. C. Haxton, (1979). *Multipole operators in semileptonic weak and electromagnetic interactions with nuclei.* Atomic Data and Nuclear Data Table, Vol. 23, 103-176.
[9] Javier Menéndez, private communication